Sensors and Actuators B 221 (2015) 673–680

Contents lists available at ScienceDirect

Sensors and Actuators B: Chemical

journal homepage: www.elsevier.com/locate/snb

Mixed potential type acetone sensor using stabilized zirconia and $M_3V_2O_8$ (M: Zn, Co and Ni) sensing electrode

Fangmeng Liu, Yehui Guan, Ruize Sun, Xishuang Liang*, Peng Sun, Fengmin Liu, Geyu Lu*

State Key Laboratory on Integrated Optoelectronics, College of Electronic Science and Engineering, Jilin University, 2699 Qianjin Street, Changchun 130012, China

ARTICLE INFO

Article history:
Received 25 April 2015
Received in revised form 30 June 2015
Accepted 4 July 2015
Available online 6 July 2015

Keywords:
Acetone sensor
YSZ
Mixed potential
$Zn_3V_2O_8$

ABSTRACT

A series of mixed potential type gas sensors using stabilized zirconia and $M_3V_2O_8$ (M: Zn, Co and Ni) sensing electrode were fabricated and applied for detecting acetone at 600 °C. Among the sensors utilizing these composite oxides ($Zn_3V_2O_8$, $Co_3V_2O_8$ and $Ni_3V_2O_8$)–SEs prepared via a facile sol–gel method, the sensor attached with $Zn_3V_2O_8$–SE exhibited the highest response to acetone at 600 °C. Therefore, the present study mainly focused on acetone sensing performance for YSZ-based sensor using $Zn_3V_2O_8$–SE at 600 °C. Results showed that the sensor attached with $Zn_3V_2O_8$–SE could detect even 1 ppm acetone with an acceptable response. Moreover, ΔV of the sensor attached with $Zn_3V_2O_8$–SE exhibited segmentally linear relationship to the logarithm of acetone concentration in the ranges of 1–10 ppm and 10–400 ppm, which the sensitivities were −16 and −56 mV/decade, respectively. The present device also displayed good repeatability, small drifts in 30 days measured period, and the excellent sensitivity and relatively good selectivity in the presence of various interfering gases before and after 30 days high-temperature-aging of 600 °C. Additionally, polarization curve was measured to further demonstrate the mixed potential mechanism.

1. Introduction

Acetone is regarded as one of the important raw material, solvent and flammable gases due to its chemical activity and relative cheapness, which is extensively used in many fields of industrial production. However, many health problems, such as headache, fatigue and harmfulness to nerve system and visceral organs, will be caused when the concentration of inhalation is higher than 173 ppm [1,2]. In addition, the medical reports indicate a large quantity of acetone is generated in the bodies of diabetic patients and the acetone concentration in plasma is approximately two orders of magnitude higher than that of common person. Acetone has been classified as an important breath biomarker or accessorial tool for noninvasive diagnosis of human type-1 diabetes [3–5]. Therefore, acetone sensors with high sensitivity, quick response–recovery, good selectivity and stability have been the focus of worldwide research for human health and safety.

In recent years, the different kinds of acetone sensors based on different sensing mechanism have been designed and fabricated by many research groups. Among them, some oxide semiconductor acetone sensors reported are either relative poor sensitivity or selectivity [6–9]. Therefore, sensors based on solid electrolyte have received steadily growing attentions for their excellent sensing performance, chemical/physical reliability, miniaturization potential and low fabrication cost. So far, several solid-electrolyte type acetone sensors using different oxide electrode materials have been reported. Lu et al. fabricated the mixed-potential-type acetone sensors using NASICON solid electrolyte and different Cr-based spinel oxide sensing electrodes, which exhibit effective response to acetone and the improvement of the sensing performance for the sensor by increasing the length of three-phase-boundary (TPB) [10]. Kasalizadeh et al. reported Yttria-stabilized zirconia (YSZ)-based sensors using coupled metal oxide-doped Pt/SnO_2 sensing electrodes, such as SiO_2, MoO_3, Sm_2O_3 and CeO_2, result in the good response and lower response and recovery times [11]. Based on these, the selection of a proper oxide electrode material is critically important for the sensing performance of the sensor. Thus, the design and development of low cost, simple synthesis process and high-performance novel oxide sensing electrode materials for YSZ-based acetone sensors with good sensitivity, selectivity and stability still are urgently needed.

In this study, novel type $M_3V_2O_8$ (M: Zn, Co and Ni) composite oxide materials are prepared via a facile sol–gel method and

* Corresponding authors.
E-mail addresses: liangxs@jlu.edu.cn (X. Liang), lugy@jlu.edu.cn (G. Lu).

http://dx.doi.org/10.1016/j.snb.2015.07.023
0925-4005/

are used as sensing electrode for fabricating YSZ-based mixed-potential-type sensor, which can be used to detect acetone. The results indicate the sensor using $Zn_3V_2O_8$ composite oxide material as sensing electrode shows the highest response to acetone. The gas sensing properties including response, repeatability, selectivity and stability for the sensor attached with $Zn_3V_2O_8$–SE to acetone are systematically investigated and the sensing mechanism is discussed. To the best of our knowledge, this is the first example to utilize $Zn_3V_2O_8$ composite material as sensing electrode for YSZ-based sensor for the detection of acetone.

2. Experimental

2.1. Preparation and characterization of $M_3V_2O_8$ sensing electrode materials

The $Zn_3V_2O_8$ was prepared from zinc nitrate hexahydrate ($Zn(NO_3)_2{\cdot}6H_2O$), ammonium metavanadate (NH_4VO_3), glycine (Gly), and ethylene glycol (EG) by the sol–gel method [12]. In a typical process, $Zn(NO_3)_2{\cdot}6H_2O$ and stoichiometric NH_4VO_3 (the molar ratio of Zn/V = 3:2) were dissolved in deionized water, respectively. Gly was added into the NH_4VO_3 solution (the molar ratio of Gly/V = 4:1) and stirred at 60 °C for 2 h to obtain a yellow transparent solution. EG and $Zn(NO_3)_2$ solution were dropwise added into the mixture described above and then stirred at 90 °C until to a gel solution was obtained. The resultant solution was maintained at 80 °C for 12 h at electric vacuum drying oven. The precursor gel was then sintered at 750 °C for 4 h in muffle furnace by a gradual increase of temperature to get inchoate samples. In order to obtain a uniform crystalline phase, the inchoate samples obtained were added into ethanol solution, respectively and were stirred in room temperature for 4 h, then raided the temperature to 80 °C until the ethanol solution was completely removed. Finally, the sample was sintered at 750 °C for 4 h in muffle furnace by a gradual increase of temperature and a yellowish powder of $Zn_3V_2O_8$ was obtained. The $M_3V_2O_8$ (M: Co and Ni) composite oxide materials were prepared by the sol–gel method according to the procedure previously described in Ref. [13].

X-ray diffraction (XRD) patterns of SE materials were measured by Rigaku wide-angle X-ray diffractometer (D/max rA, using Cu Kα radiation at wave length = 0.1541 nm) in the range of 10–80°. Field-emission scanning electron microscopy (FESEM) observations of surface morphology of the $M_3V_2O_8$–SE materials were obtained using a JEOL JSM-7500F microscope with an accelerating voltage of 15 kV.

2.2. Fabrication and measurement of gas sensor

The sensor was fabricated using the YSZ plate (8 mol% Y_2O_3-doped, 2 mm × 2 mm^2, 0.2 mm thickness, provided by Tosoh Corp., Japan). A point-shaped and a narrow stripe-shaped Pt electrode (reference electrode, RE) were formed on two ends of the YSZ plate using a commercial Pt paste (Sino-platinum Metals Co., Ltd.). The various sensing materials obtained were mixed with a minimum quantity of deionized water, respectively. The resultant paste was then applied on the point-shaped Pt to form stripe-shaped SE. The Pt heater formed on Al_2O_3 substrate was then attached to the YSZ plate by the inorganic adhesive, which provided the required heating temperature for the sensor. The schematic diagram of the sensor was shown in Fig. 1.

The gas sensing characteristics of the fabricated sensors were measured by a conventional static method [14,15]. The electric potential difference (V) between the SE and the RE was measured with a digital electrometer (Rigol Technologies, Inc., DM3054, China) when the sensor was exposed to air or sample gas. The

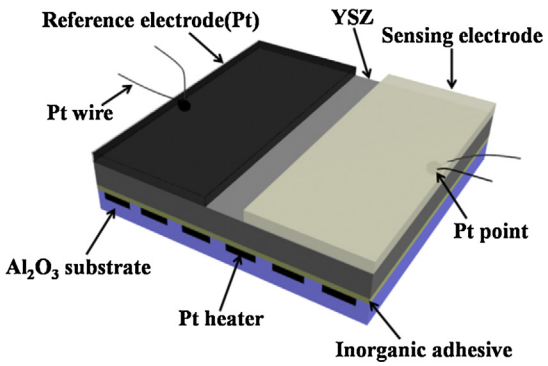

Fig. 1. Schematic diagram of the sensor.

results obtained were recorded with a computer connected to the electrometer [16]. The desired concentration of sample gas was obtained by the static liquid gas distribution method, which was calculated by the following formula [17,18],

$$C = \frac{22.4 \times \rho \times \varphi \times V_1}{M \times V_2} \times 1000$$

where, C (ppm) is the desired target gas concentration; ρ (g/mL) the density of the liquid; φ the required gas volume fraction; V_1 (μL)and V_2 (L) the volume of the liquid and chamber, respectively; and M (g/mol) the molecular weight of the liquid. The current–voltage (polarization) curves of the sensor were carried out by means of the potentiodynamic method (CHI600C, Instrument corporation of Shanghai, China) using a two-electrode configuration in the base gas (air) and the sample gas (200 ppm acetone + air) at 600 °C.

3. Results and discussion

The crystalline structure of the product prepared was identified by X-ray diffraction (XRD). Fig. 2(a) reveals the XRD pattern of $Zn_3V_2O_8$ composite oxide material. All the diffraction peaks for $Zn_3V_2O_8$ matched well with those of standard XRD patterns of the orthorhombic structure of $Zn_3V_2O_8$ oxide, which agreed well with the reported values from the Joint Committee on Powder Diffraction Standards card (JCPDS#34-0378). The sharp diffraction peaks also suggested the good crystallinity of the prepared $Zn_3V_2O_8$ composite oxide sensing electrode material. Additionally, it can be seen, from Fig. 2(b), that the as-prepared other oxide ($Ni_3V_2O_8$ and $Co_3V_2O_8$) show good agreement with the Joint Committee on Powder Diffraction Standards cards $Ni_3V_2O_8$ (JCPDS#74-1484) and $Co_3V_2O_8$ (JCPDS#74-1486), respectively. The morphologies of $M_3V_2O_8$ sensing electrode materials were characterized by FESEM. The low magnification FESM image of Fig. 3(a) revealed that the $Zn_3V_2O_8$ sensing electrode shows a loose and porous morphology, which the pore size is roughly 2 μm. It can be observed that, from Fig. 3(b), $Zn_3V_2O_8$ is composed of particles with the rough size in the range of 1–4 μm. Furthermore, the EDS mapping images of the surface of $Zn_3V_2O_8$ sensing electrode layer are shown in Fig. 3(c–f). For the $Zn_3V_2O_8$ sensing electrode layer, as can be seen, the signals of Zn, V, O were detected on the surface of material. The SEM images of $M_3V_2O_8$ (M: Co and Ni) in Fig. 3(g and h) indicated that the $Co_3V_2O_8$ and $Ni_3V_2O_8$ sensing electrode materials also showed porosity of morphology with the rough size of 1 and 0.5 μm, and the particle size was roughly in the range of 1–4 and 0.2–2 μm.

The response of the sensor attached with $M_3V_2O_8$ (M: Zn, Co and Ni) as sensing electrode materials to 200 ppm acetone were measured and shown in Fig. 4. It is clearly seen that the sensor utilizing $Zn_3V_2O_8$–SE exhibited the highest response value (−82.5 mV) comparing with the device attached with other oxide materials as sensing electrodes. The acetone sensing mechanism for the

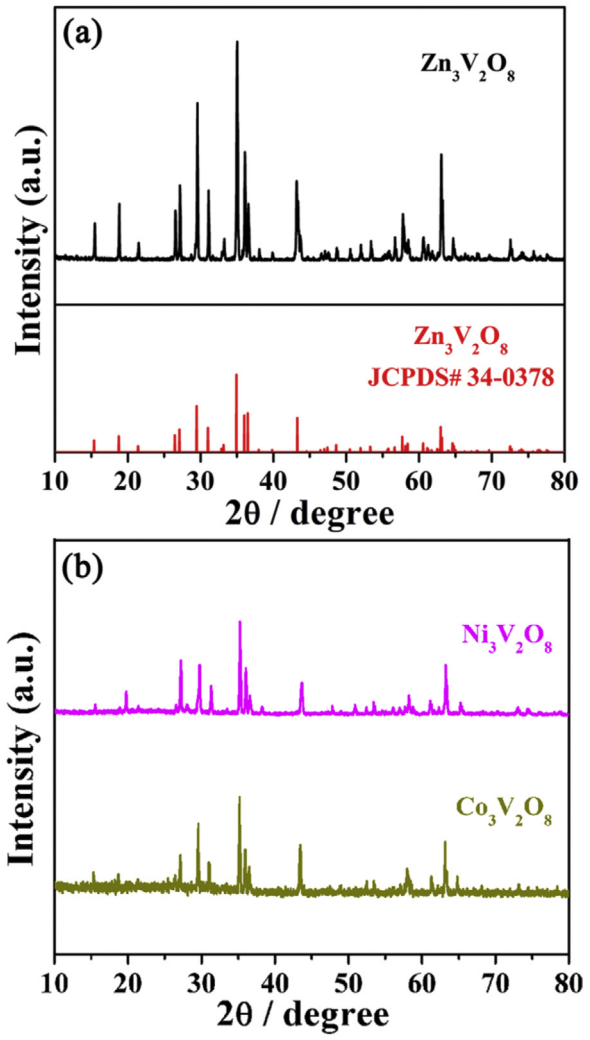

Fig. 2. (a) XRD pattern of $Zn_3V_2O_8$ composite oxide material; (b) XRD pattern of $M_3V_2O_8$ (M: Ni and Co) oxide materials.

sensor attached with $M_3V_2O_8$–SEs was based on mixed potential type theory [19–21]. For acetone atmosphere, the acetone gas passed through the electrode layer and reached the triple-phase-boundary (TPB) of SE/YSZ/acetone gas. And then, the following two electrochemical reactions proceed simultaneously at the TPB and consequently formed a local cell at the SE. When the rates of the cathodic (1) and anodic reaction (2) are equal to each other, the dynamic equilibrium is reached, and the electrode potential is the mixed potential. The difference of the sensing electrode and reference electrode potentials is measured as the sensing signal.

$$\text{Cathodic}: O_2 + 4e^- \rightarrow 2O^{2-} \quad (1)$$

$$\text{Anodic}: 1/4\,C_3H_6O + 2O^{2-} \rightarrow 3/4CO_2 + 3/4H_2O + 4e^- \quad (2)$$

The sensing signal intensity is determined by the rates of electrochemical reactions (1) and (2), nevertheless, the rates of electrochemical reaction are strongly dependent on the micro-morphology structure of electrode materials. Therefore, as shown in Fig. 3, the reason for the different response of the sensor using $M_3V_2O_8$–SEs may be attributed to the different micro-morphologies of sensing electrode materials. The $Zn_3V_2O_8$–SE material exhibited the largest pore size, comparing with that of other two oxide materials. This porosity of sensing electrode material with the larger pore size could provide the relatively superior diffusion channels to acetone gas and accelerated the diffusion in sensing electrode layer and reduced the acetone consumption in the process of the spread of sensing electrode layer. This will ensure that large quantities of acetone gases smoothly reach to the TPB and participate in the electrochemical reaction to the point of largest response. Additionally, the $Zn_3V_2O_8$ oxide material showed an improved conductivity and electrochemical capacity [22–24]. Based on these excellent properties, it was beneficial to the electron transport, which could accelerate the electrochemical reaction (2) and result in the highest response value. In order to further clarify the reason for the highest response of the sensor utilizing $Zn_3V_2O_8$–SE and validate the proposed mixed-potential model, the polarization curves in air and 200 ppm acetone for the sensors attached with $M_3V_2O_8$ (M: Zn, Co and Ni)–SEs at 600 °C were measured and shown in Fig. 5. The cathodic polarization curve was obtained in air, and the anodic polarization curve was obtained by subtracting in air from in sample gas (200 ppm acetone + air). It is clearly seen that the sensor attached with $Zn_3V_2O_8$–SE exhibited the highest electrochemical catalytic activity to anodic reaction of acetone, by comparing the anodic polarization curves of the sensors using $M_3V_2O_8$ (M: Zn, Co and Ni)–SEs. In this case, the sensor attached with $Zn_3V_2O_8$–SE gave rise to the highest response to acetone in the examined concentration at 600 °C. Therefore, we paid considerable attention to the sensor based on $Zn_3V_2O_8$–SE. Additionally, the mixed potential can be estimated from the intersection of the cathodic and anodic polarization curves [25–28]. Based on the comparison of the mixed potential estimated values and the potential difference values experimentally observed for fabricated three devices, in Table 1. The estimated values (−52, −43 and −80.5 mV) for the sensor attached with $Co_3V_2O_8$, $Ni_3V_2O_8$, and $Zn_3V_2O_8$ as SE are in close proximity to those observed values (−54, −44 and −82.5 mV). These coincidences indicate that the present sensors conform to the mixed-potential mechanism.

It is well known that the response of the sensor depended strongly on the operation temperature. Therefore, the optimal operating temperature of the sensor attached with $Zn_3V_2O_8$–SE to acetone was investigated. The response and recovery transients for the sensor using $Zn_3V_2O_8$–SE to 100 ppm acetone at different operating temperatures are exhibited in Fig. 6. It can be observed that the response to 100 ppm acetone for fabricated sensor tended to increase initially with the increasing of the operating temperature and the highest response value was obtained at 600 °C. Above 600 °C, the response of the sensor tended to decrease. The occurrence of the electrochemical reaction for the present device at TPB needed definite activation energy [29]. The electrochemical reaction did not gain enough activation energy at below 600 °C, thus, the sensitivity of the sensor to acetone increased with the increasing of temperature. However, the desorption process of acetone exhibited dominant at above 600 °C, and the amount of acetone adsorbed on the SE became less and less along with the increasing temperature. Hence, the sensitivity of the sensor to acetone decreased with further increases in operating temperature. Consequently, the optimal operating temperature for the present sensor was considered to be 600 °C. As we known, the MOS based sensors can work at operating temperature below 400 °C, which reduce power consumption. But, compared with reported [6,30–34], the present sensor fabricated has the advantages of relative small shifts

Table 1
Comparison of the mixed potential estimated and the potential difference value observed for the sensors using $M_3V_2O_8$ (M: Zn, Co and Ni)–SEs to 200 ppm acetone at 600 °C.

Sensor	Acetone Conc. (ppm)	Mixed potential (estimated) (mV)	Potential difference value (observed) (mV)
$Co_3V_2O_8$–SE	200	−52	−54
$Ni_3V_2O_8$–SE	200	−43	−44
$Zn_3V_2O_8$–SE	200	−80.5	−82.5

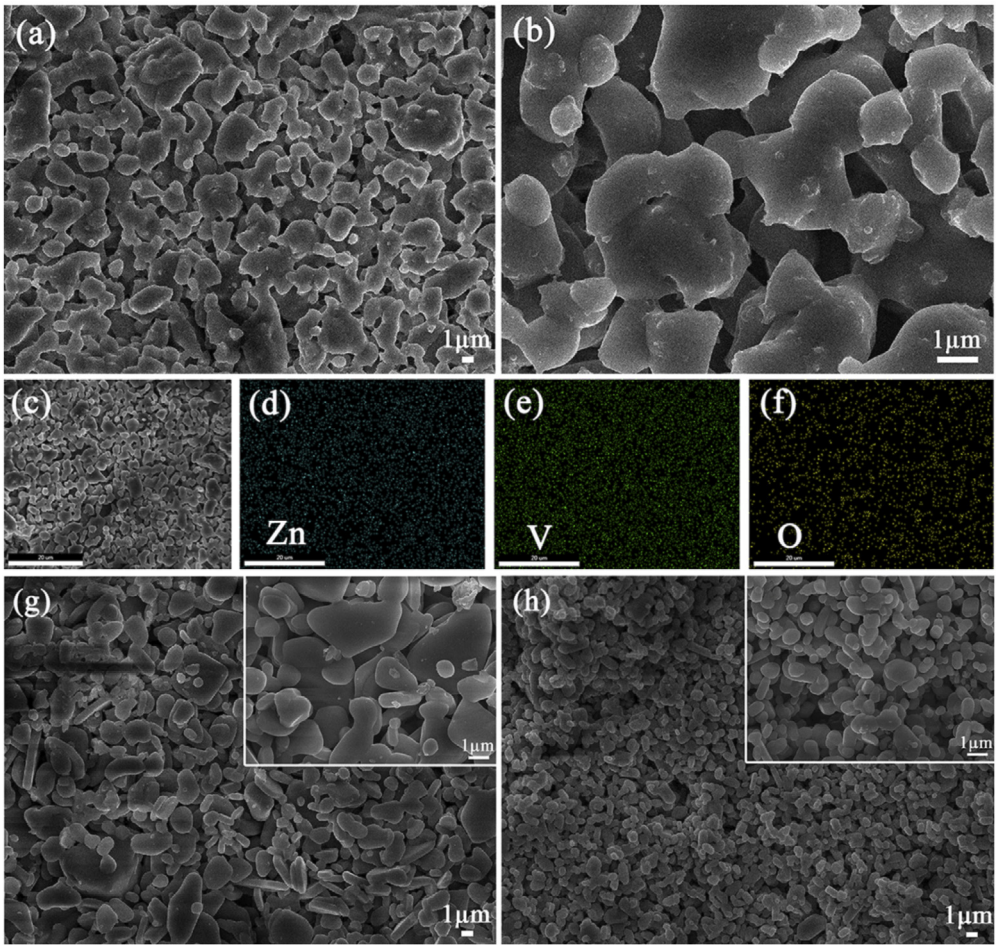

Fig. 3. (a and b) SEM images of $Zn_3V_2O_8$ sensing electrode material; (c–f) EDS mapping images of the surface of $Zn_3V_2O_8$–SE; (g and h) SEM images of $M_3V_2O_8$ (M: Co and Ni) sensing electrode materials.

in long-term stability tested period, large sensitivity and relative short response and recovery times to acetone. These factors are beneficial to ensure the accuracy of the detection in the process of practical application. Based on the viewpoint of low energy consumption, however, the development of high performance and low power consumption mixed potential type gas sensor by developing new type electrode materials and designing new device structure still need to devote more in our future work.

The response transients curve for the YSZ-based sensor attached with $Zn_3V_2O_8$–SE toward different concentrations of acetone in the range of 10–400 ppm was examined at 600 °C and the results obtained are shown in Fig. 7(a). It is seen that the response of the present sensor to acetone reached the steady-state value in a short time in the range of measured concentrations. The typical 90% response time for the sensor using $Zn_3V_2O_8$–SE toward 50 and 100 ppm acetone are approximately 34 and 27 s, respectively. The

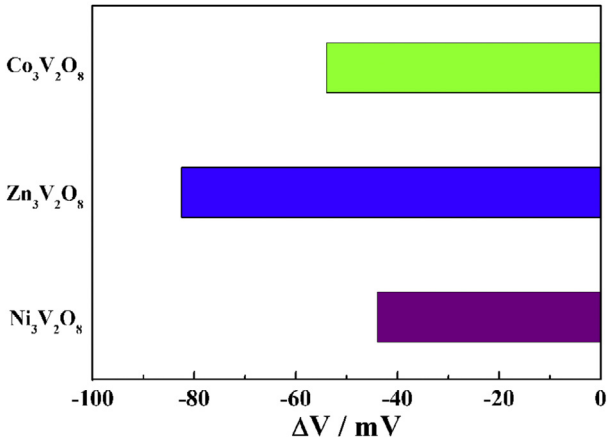

Fig. 4. Response of the sensors to 200 ppm acetone attached with different materials as sensing electrode at 600 °C.

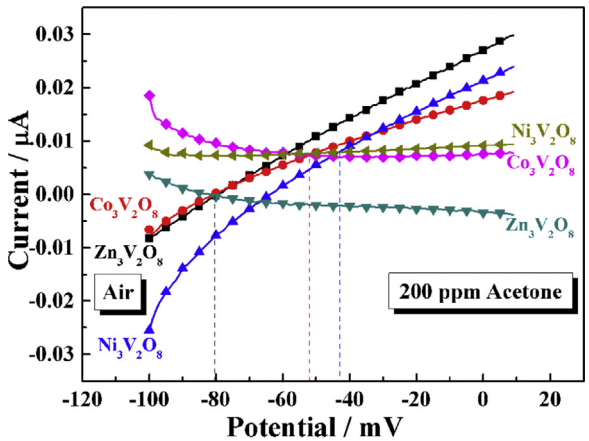

Fig. 5. Polarization curves in air and 200 ppm acetone for the sensors attached with $M_3V_2O_8$ (M: Zn, Co and Ni)–SEs at 600 °C.

Table 2
Comparison of the sensing performance of the present sensor and that of devices reported in literatures.

Material	Acetone concentration (ppm)	Response (mV)	Sensitivity (slope) (mV/decade)	Reference
$Zn_3V_2O_8$	100	−69	−56	Present work
$NiCr_2O_4$	100	−60	−22	[10]
SnO_2	100	22	45	[11]
$Pt/CeO_2/SnO_2$	100	19	36	[11]
α-Fe_2O_3 nanoparticle	100	22.4 ($R = R_{acetone}/R_{air}$)	–	[30]
ZnO	100	10.5 ($R = R_{acetone}/R_{air}$)	–	[31]
Porous $ZnO/ZnCO_2O_4$	100	7.5 ($R = R_{acetone}/R_{air}$)	–	[35]

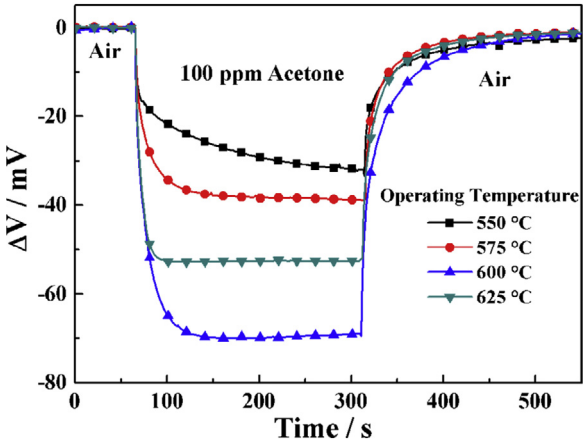

Fig. 6. Response and recovery transients for the sensor using $Zn_3V_2O_8$–SE to 100 ppm acetone at different operating temperatures.

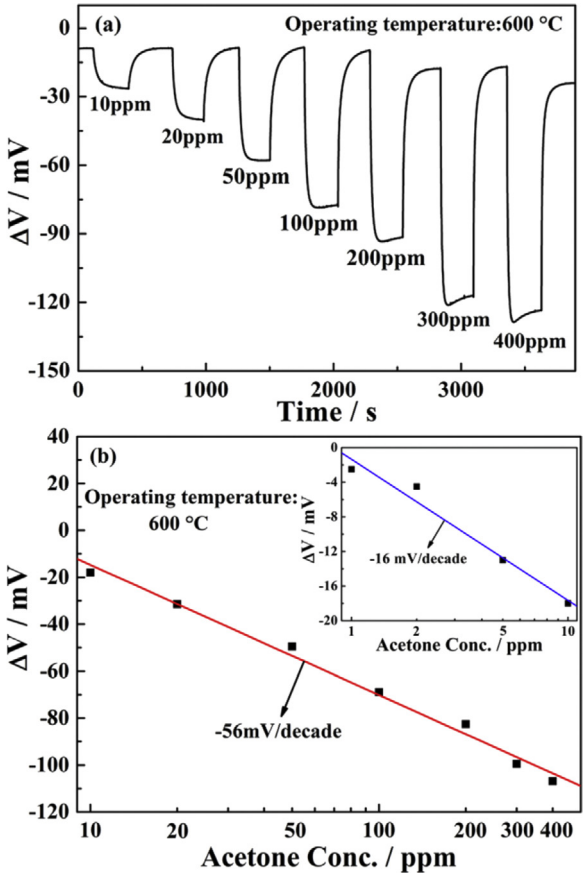

Fig. 7. (a) Response transients curve for the YSZ-based sensor attached with $Zn_3V_2O_8$–SE toward different concentrations of acetone in the range of 10–400 ppm at 600 °C; (b) dependence of ΔV on the acetone concentration for the sensor attached with $Zn_3V_2O_8$–SE at 600 °C.

response for the sensor attached with $Zn_3V_2O_8$–SE to 100 ppm acetone at 600 °C was still as large as −69 mV. The dependence of ΔV on the acetone concentration for the sensor attached with $Zn_3V_2O_8$–SE at 600 °C is depicted in Fig. 7(b). In this case, almost a linear relationship between the ΔV and the logarithm of acetone concentration in the examined range of 10–400 ppm at 600 °C was observed, which conforms to mixed potential type sensor. The sensitivity of the fabricated sensor was −56 mV/decade. The comparison of the acetone sensing property for the current fabricated sensor and that reported previously in literature is presented in Table 2. Obviously, the sensor using $Zn_3V_2O_8$–SE exhibited better sensing performance to acetone than previously reported devices. Moreover, the ΔV for the present sensor to acetone in the range of 1–10 ppm was also measured at 600 °C and the result obtained is shown in the inset of Fig. 7(b). It is surprising that the sensor attached with $Zn_3V_2O_8$–SE could detect even 1 ppm acetone with an acceptable response (−2.5 mV). In this case, the ΔV also varied linearly with acetone concentration in the range of 1–10 ppm and the slope was significantly lower than that of high concentration range, which is −16 mV/decade. The reason for the occurrence of such a linear dependence of acetone sensitivity in the low concentration range is may be followed. As known very well, the electrochemical reaction for the present fabricated sensor occurred at the TPB. And the sensing signal of the sensor depended on the concentration of acetone at TPB of SE and the amount of active sites of TPB. For the low concentration range of acetone (1–10 ppm), the amount of TPB active sites for the sensor attached with $Zn_3V_2O_8$–SE are enough to provide the electrochemical reaction, thereby, the sensitivity of the sensor are mainly related to the amount of acetone, which reached the TPB of SE and participated in the electrochemical reaction [36,37]. When the sensor is exposed to the acetone atmosphere, the acetone gas need pass through the sensing electrode layer and reach the TPB, which participate in the electrochemical reaction. Although with a porosity structure for the SE, a certain amount of gas was still consumed in the process of diffusion through the $Zn_3V_2O_8$–SE layer. When the concentration of the measured acetone is at a lower level (1–10 ppm), the acetone consumption in the process of diffusion accounted for the proportion of the total quantity of acetone is larger than that of higher acetone concentration (10–400 ppm). Therefore, the relatively low sensitivity to acetone concentration in the range of 1–10 ppm was observed.

The continuous response–recovery transients of the sensor attached with $Zn_3V_2O_8$–SE to 50 ppm acetone at 600 °C had been measured, as illustrated in Fig. 8. It is clearly seen that the potential difference response to 50 ppm acetone and air for fabricated sensor was effectively reproduced in the examined ten-time cycles, which was confirmed that the sensor exhibited good repeatability. Additionally, the selectivity and stability for a gas sensor are important sensing performance parameters, Fig. 9 shows the cross-sensitivities for the sensor attached with $Zn_3V_2O_8$–SE at 600 °C to various gases, such as ethanol, toluene, methanol, NO_2, etc. It can be seen that the present sensor exhibited an obvious response to 50 and 100 ppm acetone, and less effective response to any other tested gases. Moreover, the response of the sensor to 50 ppm

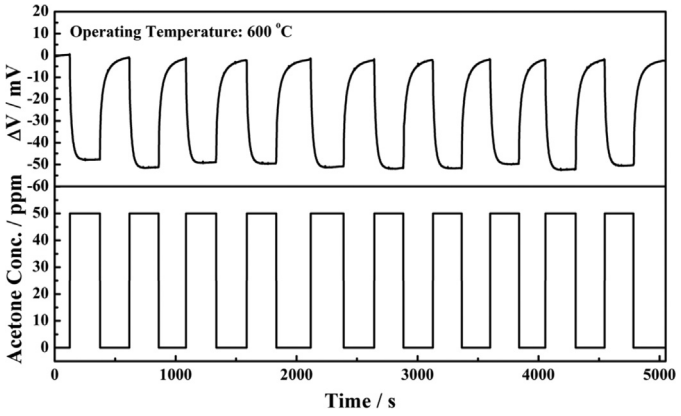

Fig. 8. Continuous response–recovery transients to 50 ppm acetone for the sensor attached with $Zn_3V_2O_8$–SE at 600 °C.

acetone was clearly higher than that to 100 ppm other gases. Furthermore, the fabricated device was evaluated in the coexisting gases of 50 ppm acetone in conjunction with other interfering gases, such as ethanol, toluene, isooctane, and CO at 600 °C. Based on the comparison of the response value of the sensor to mixture gases and 50 ppm of pure acetone, there was relatively small change from −11.5% to 7.1%. Therefore, it was concluded that the sensor using $Zn_3V_2O_8$–SE showed good selectivity to acetone as oppose to any other gases. The long-term stability to 50 ppm and 100 ppm acetone for the sensor attached with $Zn_3V_2O_8$–SE at 600 °C is shown in Fig. 10. The change amplitude of the ΔV for the sensor attached with $Zn_3V_2O_8$–SE changed slightly to 50 and 100 ppm acetone during the 30 days measurement period. In order to further illustrate exactly the change amplitude of the ΔV with time, the change of the ΔV (ΔV_s) for the sensor is given by $\Delta V_s = [(\Delta V_n - \Delta V_0)/\Delta V_0 \times 100\%]$, where ΔV_n and ΔV_0 denote the ΔV of the sensor on the n and 0 day, respectively. The results showed that the ΔV_s for the sensor to 50 and 100 ppm acetone on the 30th day were −3.0% and −10.1%, respectively. Therefore, the present fabricated sensors showed relatively good stability. Furthermore, the sensitivity and selectivity for the sensor attached with $Zn_3V_2O_8$–SE after 30 days high-temperature-aging of 600 °C were investigated and shown in Fig. 11. It was found that, from Fig. 11(a), the sensitivity of the fabricated sensor after 30 days high-temperature-aging decreased −2 and −9 mV/decade to acetone concentration in the range of 1–10 and 10–400 ppm at 600 °C, comparing with that of device before aging. It can be seen that, in Fig. 11(b), the device after 30 days aging also exhibited an obvious response to acetone, and less effective response to any other

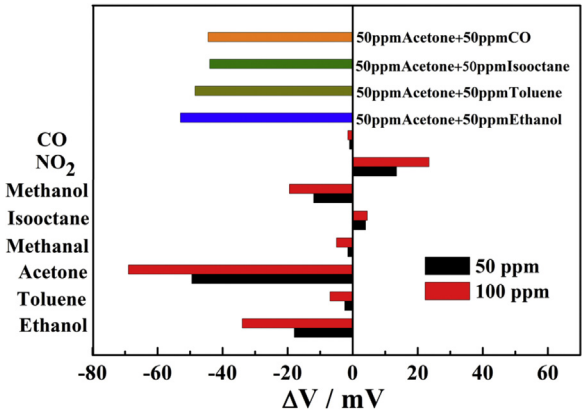

Fig. 9. Cross-sensitivities for the sensor attached with $Zn_3V_2O_8$–SE to various gases at 600 °C.

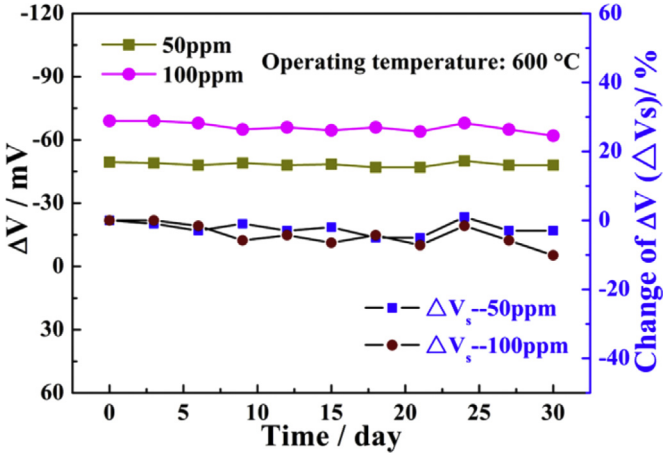

Fig. 10. Long-term stability to 50 ppm and 100 ppm acetone for the sensor attached with $Zn_3V_2O_8$–SE at 600 °C.

tested gases. Moreover, the effect of the ethanol as coexistence gas on acetone response for the fabricated sensor could not be ignored. By comparing the response value of the sensor to mixture gases (50 ppm acetone + 50 ppm ethanol) and 50 ppm of pure acetone, the change of response was 18%. The improvement of selectivity to ethanol remains to be further investigated in the future work. On the whole, the present sensor still displayed selectivity to various interfering gases and excellent sensitivity to acetone even at elevated temperature for a long term that after 30 days.

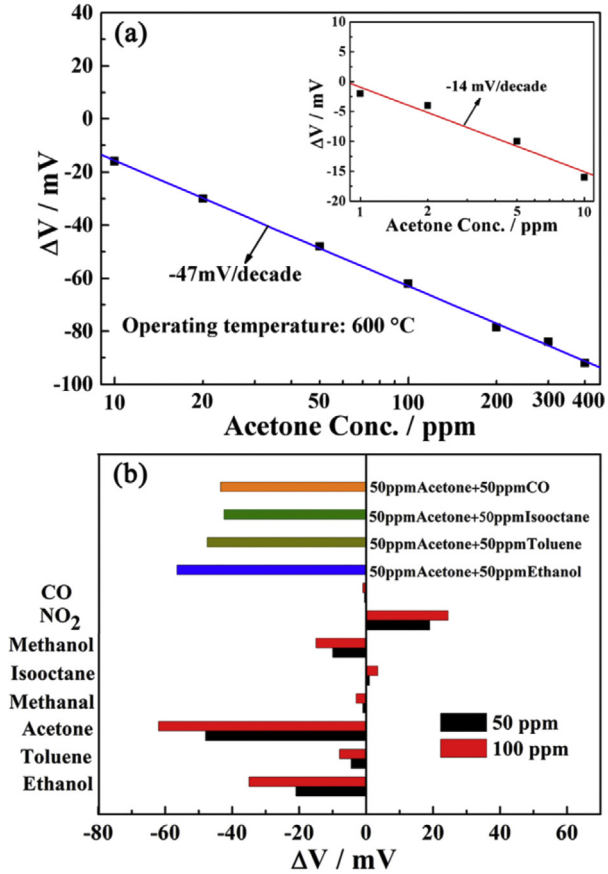

Fig. 11. (a) Dependence of ΔV on the acetone concentration for the sensor attached with $Zn_3V_2O_8$–SE on the 30th day of examination at 600 °C; (b) cross-sensitivities for the sensor attached with $Zn_3V_2O_8$–SE to various gases on the 30th day of examination at 600 °C.

4. Conclusion

In summary, mixed potential type YSZ-based electrochemical gas sensors using $M_3V_2O_8$ (M: Zn, Co, and Ni) as sensing electrode were fabricated to detect acetone at the operating temperature of 600 °C. Three kinds of $M_3V_2O_8$ were prepared by sol–gel method and their sensing properties were investigated. Among these complex oxides evaluated, $Zn_3V_2O_8$ was found to be most applicable to the sensing electrode for the YSZ-based sensor to detect acetone. The result indicated that the sensor attached with $Zn_3V_2O_8$–SE exhibited large response (−69 mV) to 100 ppm acetone and sensitivity (−56 mV/decade) to acetone concentration in the range of 10–400 ppm at 600 °C. The low detection limit for present sensor was 1 ppm to acetone. Additionally, the fabricated sensor displayed the excellent stability in 30 days measurement period, and good sensitivity and selectivity after 30 days high-temperature-aging of 600 °C. Based on these remarkable sensing characteristics, the present sensor showed the potential application value for detecting acetone in atmosphere and diabetes.

Acknowledgements

This work is supported by Application and Basic Research of Jilin Province (20130102010JC), the National Nature Science Foundation of China (Nos. 61134010, 61327804, 61374218, 61377058 and 61473132), Program for Chang Jiang Scholars and Innovative Research Team in University (No. IRT13018) and National High-Tech Research and Development Program of China (863 Program, Nos. 2013AA030902 and 2014AA06A505).

References

[1] Q. Jia, H. Ji, Y. Zhang, Y. Chen, X. Sun, Z. Jin, Rapid and selective detection of acetone using hierarchical ZnO gas sensor for hazardous odor markers application, J. Hazard. Mater. 276 (2014) 262–270.
[2] L. Wang, A. Teleki, S. Pratsinis, P. Gouma, Ferroelectric WO_3 nanoparticles for acetone selective detection, Chem. Mater. 20 (2008) 4794–4796.
[3] P. Sun, Y. Cai, S. Du, X. Xu, L. You, J. Ma, F. Liu, X. Liang, Y. Sun, G. Lu, Hierarchical α-Fe_2O_3/SnO_2 semiconductor composites: hydrothermal synthesis and gas sensing properties, Sens. Actuators B: Chem. 182 (2013) 336–343.
[4] C. Deng, J. Zhang, X. Yu, W. Zhang, X. Zhang, Determination of acetone in human breath by gas chromatography-mass spectrometry and solid-phase microextraction with on-fiber derivatization, J. Chromatogr. B 810 (2004) 269–275.
[5] T. Xiao, X. Wang, Z. Zhao, L. Li, L. Zhang, H. Yao, J. Wang, Z. Li, Highly sensitive and selective acetone sensor based on C-doped WO_3 for potential diagnosis of diabetes mellitus, Sens. Actuators B: Chem. 199 (2014) 210–219.
[6] S. Choi, I. Lee, B. Jang, D. Yong, W. Ryu, C. Park, I. Kim, Selective diagnosis of diabetes using Pt-functionalized WO_3 hemitube networks as a sensing layer of acetone in exhaled breath, Anal. Chem. 85 (2013) 1792–1796.
[7] M. Righettoni, A. Tricoli, S. Pratsinis, Si:WO_3 sensors for highly selective detection of acetone for easy diagnosis of diabetes by breath analysis, Anal. Chem. 82 (2010) 3581–3587.
[8] T. Nasution, I. Nainggolan, S. Hutagalung, K. Ahmad, Z. Ahmad, The sensing mechanism and detection of low concentration acetone using chitosan-based sensor, Sens. Actuators B: Chem. 177 (2013) 522–528.
[9] L. Tang, Y. Li, K. Xu, X. Hou, Y. Lv, Selective acetone sensor based on its cataluminescence from nano-La_2O_3 surface, Sens. Actuators B: Chem. 132 (2008) 243–249.
[10] H. Zhang, C. Yin, Y. Guan, X. Cheng, X. Liang, G. Lu, NASICON-based acetone sensor using three-dimensional three-phase boundary and Cr-based spinel oxide sensing electrode, Solid State Ionics 262 (2014) 283–287.
[11] M. Kasalizadeh, A. Khodadadi, Y. Mortazavi, Coupled metal oxide-doped Pt/SnO_2 semiconductor and yittria-stabilized zirconia electrochemical sensors for detection of VOCs, J. Electrochem. Soc. 160 (2013) B218–B224.
[12] T. Li, Z. Honda, T. Fukuda, J. Luo, N. Kamata, Fabrication and characterization of $Zn_3V_2O_8$ phosphor by sol–gel process, J. Sol–Gel. Sci. Technol. 66 (2013) 225–230.
[13] F. Liu, R. Sun, Y. Guan, X. Cheng, H. Zhang, Y. Guan, X. Liang, P. Sun, G. Lu, Mixed-potential type NH_3 sensor based on stabilized zirconia and $Ni_3V_2O_8$ sensing electrode, Sens. Actuators B: Chem. 210 (2015) 795–802.
[14] X. Niu, W. Du, W. Du, Preparation and gas sensing properties of ZnM_2O_4 (M = Fe, Co, Cr), Sens. Actuators B: Chem. 99 (2004) 405–409.
[15] Q. Diao, C. Yin, Y. Guan, X. Liang, S. Wang, Y. Liu, Y. Hu, H. Chen, G. Lu, The effects of sintering temperature of $MnCr_2O_4$ nanocomposite on the NO_2 sensing property for YSZ-based potentiometric sensor, Sens. Actuators B: Chem. 177 (2013) 397–403.
[16] Q. Diao, F. Yang, C. Yin, J. Li, S. Yang, X. Liang, G. Lu, Ammonia sensor based on stabilized zirconia and $CoWO_4$ sensing electrode, Solid State Ionics 225 (2012) 328–331.
[17] H. Fan, Y. Zeng, H. Yang, X. Zheng, L. Liu, T. Zhang, Preparation and gas sensitive properties of ZnO–CuO nanocomposites, Acta Phys. Chem. Sin. 24 (2008) 1292–1296.
[18] P. Sun, X. Zhou, C. Wang, B. Wang, X. Xu, G. Lu, One-step synthesis and gas sensing properties of hierarchical Cd-doped SnO_2 nanostructures, Sens. Actuators B: Chem. 190 (2014) 32–39.
[19] N. Miura, T. Sato, S. Anggraini, H. Ikeda, S. Zhuiykov, A review of mixed-potential type zirconia-based gas sensors, Ionics 20 (2014) 901–925.
[20] G. Lu, N. Miura, N. Yamazoe, High-temperature hydrogen sensor based on stabilized zirconia and a metal oxide electrode, Sens. Actuators B: Chem. 35–36 (1996) 130–135.
[21] G. Lu, N. Miura, N. Yamazoe, High-temperature sensors for NO and NO_2 based on stabilized zirconia and spinel-type oxide electrodes, J. Mater. Chem. 7 (1997) 1445–1449.
[22] L. Gan, D. Deng, Y. Zhang, G. Li, X. Wang, L. Jiang, C. Wang, $Zn_3V_2O_8$ hexagon nanosheets: a high-performance anode material for lithium-ion batteries, J. Mater. Chem. A 2 (2014) 2461–2466.
[23] M. Wang, Y. Shi, G. Jiang, 3D hierarchical $Zn_3(OH)_2V_2O_7{\cdot}2H_2O$ and $Zn_3(VO_4)_2$ microspheres: synthesis, characterization and photoluminescence, Mater. Res. Bull. 47 (2012) 18–23.
[24] D. Wang, J. Tang, Z. Zou, J. Ye, Photophysical and photocatalytic properties of a new series of visible-light-driven photocatalysts $M_3V_2O_8$ (M = Mg, Ni, Zn), Chem. Mater. 17 (2005) 5177–5182.
[25] N. Miura, J. Wang, M. Nakatou, P. Elumalai, S. Zhuiykov, M. Hasei, High-temperature operating characteristics of mixed-potential-type NO_2 sensor based on stabilized-zirconia tube and NiO sensing electrode, Sens. Actuators B: Chem. 114 (2006) 903–909.
[26] N. Miura, G. Lu, N. Yamazoe, Progress in mixed-potential type devices based on solid electrolyte for sensing redox gases, Solid State Ionics 136–137 (2000) 533–542.
[27] N. Miura, H. Kurosawa, M. Hasei, G. Lu, N. Yamazoea, Stabilized zirconia-based sensor using oxide electrode for detection of NO_x in high-temperature combustion-exhausts, Solid State Ionics 86–88 (1996) 1069–1073.
[28] G. Lu, Q. Diao, C. Yin, S. Yang, Y. Guan, X. Cheng, X. Liang, High performance mixed-potential type NO_x sensor based on stabilized zirconia and oxide electrode, Solid State Ionics 262 (2014) 292–297.
[29] X. Liang, T. Zhong, H. Guan, F. Liu, G. Lu, B. Quan, Ammonia sensor based on NASICON and Cr_2O_3 electrode, Sens. Actuators B: Chem. 136 (2009) 479–483.
[30] Y. Cao, H. Luo, D. Jia, Low-heating solid-state synthesis and excellent gas sensing properties of alpha-Fe_2O_3 nanoparticles, Sens. Actuators B: Chem. 176 (2013) 618–624.
[31] G. Lu, X. Wang, J. Liu, S. Qiu, C. He, B. Li, W. Liu, One-pot synthesis and gas sensing properties of ZnO mesoporous architectures, Sens. Actuators B: Chem. 184 (2013) 85–92.
[32] F. Liu, X. Chu, Y. Dong, W. Zhang, W. Sun, L. Shen, Acetone gas sensors based on grapheme-$ZnFe_2O_4$ composite prepared by solvothermal method, Sens. Actuators B: Chem. 188 (2013) 469–474.
[33] X. Zhou, J. Liu, C. Wang, P. Sun, X. Hu, X. Li, K. Shimanoe, N. Yamazoe, G. Lu, Highly sensitive acetone gas sensor based on porous $ZnFe_2O_4$ nanospheres, Sens. Actuators B: Chem. 206 (2015) 577–583.
[34] H. Fan, X. Jia, Selective detection of acetone and gasoline by temperature modulation in zinc oxide nanosheets sensors, Solid State Ionics 192 (2011) 688–692.
[35] X. Zhou, W. Feng, C. Wang, X. Hu, X. Li, P. Sun, K. Shimanoe, N. Yanazoe, G. Lu, Porous ZnO/$ZnCr_2O_4$ hollow spheres: synthesis, characterization, and applications in gas sensing, J. Mater. Chem. A 2 (2014) 17683–17690.
[36] X. Liang, S. Yang, J. Li, H. Zhang, Q. Diao, W. Zhao, G. Lu, Mixed-potential-type zirconia-based NO_2 sensor with high-performance three-phase boundary, Sens. Actuators B: Chem. 158 (2011) 1–8.
[37] Y. Guan, C. Yin, X. Cheng, X. Liang, Q. Diao, H. Zhang, G. Lu, Sub-ppm H_2S sensor based on YSZ and hollow balls $NiMn_2O_4$ sensing electrode, Sens. Actuators B: Chem. 193 (2014) 501–508.

Biographies

Fangmeng Liu received his B.S. degree in 2009 from College of Chemistry, Liaocheng University and M.S. degree in 2012 from Northeast Forestry University in China. Currently he is studying for his Ph.D. degree in College of Electronic Science and Engineering, Jilin University, China.

Yehui Guan received the B.E. degree in department of electronic science and technology in 2014. He is currently studying for his M.E. Sci. degree in College of Electronic Science and Engineering, Jilin University, China.

Ruize Sun received the B.E. degree in department of electronic science and technology in 2012. He is currently studying for his M.E. Sci. degree in College of Electronic Science and Engineering, Jilin University, China.

Xishuang Liang received the B.E. degree in Department of Electronic Science and Technology in 2004. He received his Doctor's degree in College of Electronic Science

and Engineering at Jilin University in 2009. Now he is an associate professor of Jilin University, China. His current research is solid electrolyte gas sensor.

Peng Sun received his Ph.D. degree from the Electronics Science and Engineering department, Jilin University, China in 2014. Now, he is engaged in the synthesis and characterization of the semiconducting functional materials and gas sensors.

Fengmin Liu received the B.E. degree in Department of Electronic Science and Technology in 2000. She received his Doctor's degree in College of Electronic Science and Engineering at Jilin University in 2005. Now she is a professor in Jilin University, China. Her current research is preparation and application of semiconductor oxide, especial in gas sensor and solar cell.

Geyu Lu received the B.Sc. degree in electronic sciences in 1985 and the M.S. degree in 1988 from Jilin University in China and the Dr. Eng. degree in 1998 from Kyushu University in Japan. Now he is a professor of Jilin University, China. His current research interests include the development of chemical sensors and the application of the function materials.